

Knots, Symmetry, and Scattering

Omar Manuar and Dwight L. Jaggard, *Fellow, IEEE*

Abstract—We investigate the physics underlying the scattering of circularly polarized plane waves from a toroidal knot and related unknot. We find that backscattering along the axis of rotational symmetry from trefoil knots is cross polarized; copolarized backscatter is in the numerical noise. In contrast, untrefoils give appreciable backscattering cross sections for both polarizations. We also study an intermediate class of structures: *morphs*, which provides a geometrical bridge between trefoil and untrefoil.

We pursue physical insight for the depolarization associated with asymmetric objects, tracing the connection from the induced charge distribution, to the induced moments, to the polarization of the backscattered field.

Index Terms—Electromagnetic scattering, knots, symmetry, topology.

I. INTRODUCTION

KAC [1] introduced the question of whether the shape of a bell could be heard within its ringing. Similarly, we wonder whether topology will imprint a characteristic signature on scattered electromagnetic waves. In particular, we ask whether the backscattering cross sections from two topologically distinct objects are different [2].

We use the symmetric trefoil, a simple toroidal knot, and form a geometrically similar unknot, termed the untrefoil, shown in Fig. 1. We calculate the backscattering differential cross section along the axis of rotational symmetry of the trefoil (and analogous axis for the untrefoil) for linearly and circularly polarized plane waves, focussing on the latter.¹

The copolarized cross section distinguishes between the symmetric trefoil and the untrefoil [4]. From the trefoil it is numerically 25 to 30 orders of magnitude smaller than cross-polarized version. Such extremely small numbers would probably be undetectable and are consistent with the theoretical absence of polarization change—we consider it numerical noise. Untrefoils, however, produce co- and cross-polarized backscattering values comparable to each other and to the cross-polarized results for the trefoils, Fig. 2. We find that all morphs examined here, whether knotted or unknotted, give significant backscatter of both polarizations.

Manuscript received February 2, 1998; revised November 22, 2000. This work was supported in part by NATO Collaborative under Contract 930923 and in part by the Complex Media Laboratory of the University of Pennsylvania.

O. Manuar is with the Complex Media Laboratory, School of Engineering and Applied Science, University of Pennsylvania, Philadelphia, PA 19104-6314 USA. He is also with the Department of Biophysics and Biochemistry, School of Medicine, University of Pennsylvania, Philadelphia, PA 19104-6059 USA.

D. L. Jaggard is with the Complex Media Laboratory, School of Engineering and Applied Science, University of Pennsylvania, Philadelphia, PA 19104-6314 USA.

Publisher Item Identifier S 0018-926X(01)05259-0.

¹We use the term co-polarized when the scattered wave has the same polarization as the incident wave and cross-polarized when it has the opposite polarization.

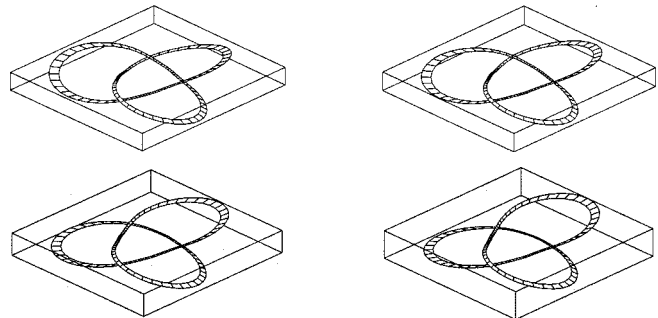


Fig. 1. We illustrate the change in geometry that accompanies a crossing switch from trefoil to untrefoil: trefoil (top left), two intermediate morphs (top right and bottom left), and associated untrefoil (bottom right). Not shown is the circular, planar loop.

It has been shown mathematically [5] that structures with less-than three-fold rotational symmetry change backscattered polarization. Here, we focus on physical insight linking shape to polarization. We use the planar loop to set up a framework, relating the charge distribution through the induced electric dipole moment to polarization. Then we discuss the trefoil, untrefoil, and morphs, calculating the electric dipole, magnetic dipole, and electric quadrupole. We also calculate the backscattering cross sections from these moments, indicating relative importance.

II. SYSTEM AND CALCULATIONS

A. Knots Studied

We briefly describe the knots and unknots used and their relationships to each other. The circular planar loop is the simplest geometry of the unknot. We use it to physically relate the polarization of the backscattering back to the induced charge distribution. This loop is continuously rotationally symmetric, the axis providing a natural direction for scattering investigations. It is related to the trefoil by symmetry and the untrefoil by topology.

A trefoil is of low knottedness: a single crossing switch changes it into an unknot² and it is a knot because it cannot become an unknot without at least one crossing change.³ Such

²When you project a knot onto a plane, you obtain a curve that may cross itself several times. Each crossing designates a point where one part of the knot passes above the other with respect to the plane. Switching above to below requires one of these parts to be broken so that the other may pass through. In the case of the trefoil, this also changes the topology, making it an unknot, specifically the untrefoil. Breaking the curve is necessary to change the topology of a knot. A knot may otherwise be geometrically deformed without changing its knottedness. It is not sufficient, however, as can be seen immediately by considering the projection of a figure-eight unknot. See, e.g., *Knots and Physics* by Louis Kauffman (Singapore, World Scientific, 1993).

³Two knots are equivalent topologically only if one can be continuously deformed into the other without breaking the curve.

a switch can be seen in the series of structures in Fig. 1⁴; they range from our standard trefoil to its related untrefoil. The trefoil is an example of a class of toroidal knots that can exist in an N -fold rotationally symmetric form. Here we choose three-fold symmetric versions as archetypal trefoils. Trefoils have topologically distinct mirror images; we don't distinguish between them because switching the handedness of both the knot and the incident radiation gives the same effect. In order to disentangle effects of topology and geometry, we also study a geometrically closely related unknot that we term an untrefoil. This is the geometry we obtained by switching a single knot crossing to unknot the trefoil; it retains much of the trefoil geometry, differing only in the region near the crossing, as defined in the projection. The untrefoil and planar loop are topologically equivalent, being different geometric forms of the unknot, but the untrefoil as defined must always be asymmetric. We also examine hybrids of trefoils and untrefoils, termed *morphs*, that demonstrate the geometries that can occur as a trefoil is changed into an untrefoil by switching a crossing. Some morphs are knotted, being trefoils topologically, but all are asymmetric like the untrefoils.

B. Backscattering Calculations

We consider knots and unknots that are formed of a thin (with a constant length to width ratio chosen in the 10^3 – 10^8 range), perfectly conducting wire. The incident radiation is a monochromatic, circularly polarized plane wave with wave vector $\mathbf{k}_{\text{inc}} \perp \hat{\mathbf{z}}$. The knot is at the origin and the rotational symmetry axis is parallel to the z -axis, Fig. 3.

We use the time-harmonic Maxwell equations and solve for the induced current and charge numerically using the method of moments (MoM) [5]. An important point is to preserve existing symmetry when dividing the structure into segments. From the incident radiation with polarization $\hat{\mathbf{e}}_0$ traveling along direction $\hat{\mathbf{n}}_0$ we calculate the scattered electric field and the differential scattering cross section, [6], [7]

$$\frac{d\sigma}{d\Omega}(\hat{\mathbf{n}}, \hat{\mathbf{e}}; \hat{\mathbf{n}}_0, \hat{\mathbf{e}}_0) = \frac{\gamma^2 |\hat{\mathbf{e}}^* \cdot \mathbf{E}_{\text{sc}}|^2}{|\hat{\mathbf{e}}^* \cdot \mathbf{E}_{\text{inc}}|^2} \quad (1)$$

of the scattered radiation with polarization $\hat{\mathbf{e}}$ along the direction $\hat{\mathbf{n}}$ normalized by the power of the incident radiation.

The copolarized backscattering in Fig. 2 shows two groups. The planar loops and trefoils fall in one category, giving only cross-polarized backscatter with co-polarization being in the noise. The untrefoils and both knotted and unknotted morphs fall into the other, giving both co- and cross-polarized backscattering. These groups are distinguished by the lack or presence of rotational symmetry. We now turn to physical reasons for these polarization differences.

⁴An example parametrization of the trefoil in spherical coordinates is $\phi = (4s\pi/3)$, $\theta = (\pi/2) + C \cos(2s\pi)$, $\rho = 2 - \sin(2s\pi) + .3 \sin^2(2s\pi) + \sin^4(\pi(s - (1/4)))$ where s is the parametric coordinate and the C is a constant determining flatness. Equations for the other structures are similar. An important point not part of the equations is to preserve existing symmetry when dividing the structure into segments.

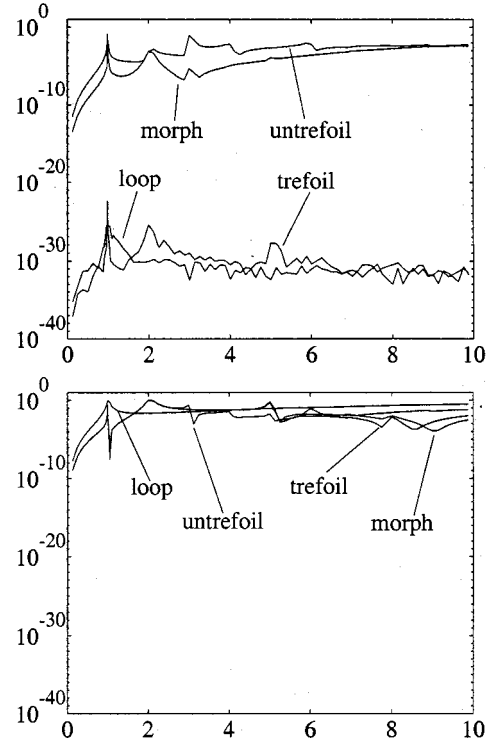


Fig. 2. Copolarized (top) and cross-polarized (bottom) backscatter cross-sections as a function of normalized length, kL , for the trefoil, untrefoil, planar loop, and morph for incident left circularly polarized radiation.

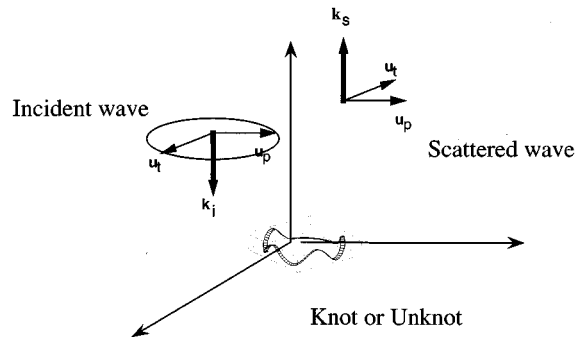


Fig. 3. Typical geometry of backscattering from knot and unknots. Here \mathbf{k}_i and \mathbf{k}_s are the incident and scattered wavevectors, respectively.

III. THE PLANAR LOOP

For physical insight, we follow the path from incident to scattered radiation. The incident field induces a time-harmonic charge distribution that can be described by its moments, each radiating its own contribution to backscattering.

Numerical calculations yield the time-harmonic induced current and charge distributions. We include the harmonic time-dependence and evaluate at time t and use the real part for the physical charge distribution, $\sigma(\mathbf{x}, t) = \text{Re}\{\sigma_0(\mathbf{x})e^{-i\omega t}\}$. We choose times over a cycle of the incident field, obtaining “snapshots.”

Plotting the value of the charge distribution along the z -axis with the loop in the plane gives a charge distribution on a loop that rotates as a unit with constant frequency and magnitude, i.e., a circularly rotating dipole (not shown). The electric dipole moment for this is in the plane of the loop and aligned with the

semi-major axis. It has the same angular frequency as the incident electric vector. Constant magnitude yields circular rotation.

Circularly rotating dipoles can be decomposed into two linearly oscillating electric dipoles of equal magnitudes in phase quadrature. Perpendicular to the plane, these dipoles give far-zone fields that are plane waves with electric vectors parallel to the dipoles. This produces an outgoing circularly polarized wave along the axis of rotation and the opposite circular polarization in the backscattering direction.

So for planar loops, the backscattering polarization is closely related to the motion of the induced charge distribution and electric dipole moment. We infer that backscattering of both polarizations is radiated when there are two dipoles, one rotating in each direction. More to the point, we conceive an idealized source of two charge distributions; each like that on a loop, but rotating in opposite directions. This simple arrangement is not the unique source, but provides a physical origin for backscattering with mixed polarization. However, such components may not be obvious by inspection of the charge distribution.

The charge distribution induced on the planar loop is qualitatively the same at all frequencies. For trefoils it is often straightforward at low frequencies to extract the direction and motion of the dipole moment. This is not the case at higher frequencies, as seen in Fig. 4. We have also observed cases in which what seems to be the motion of the charge distribution and of the dipole is inconsistent with the polarization of the backscattering. Here, examining the charge distribution is inadequate; so we calculate the electric dipole, the magnetic dipole, and electric quadrupole.

IV. CALCULATION OF MULTIPOLES

We present briefly the equations for the electric dipole, magnetic dipole, and electric quadrupole moments [8] and for the scattering cross-section term from each. The latter are useful for evaluating the relative importance of the multipoles to the general backscattering cross section.

The electric and magnetic dipole moments, \mathbf{p} and \mathbf{m} , are defined as

$$\mathbf{p}(t) = \int_{V'} \mathbf{x}' \sigma(\mathbf{x}', t) d\mathbf{x}' \quad \mathbf{m}(t) = \int_{V'} \mathbf{x}' \times \mathbf{J}(\mathbf{x}', t) d\mathbf{x}'. \quad (2)$$

Here \mathbf{x}' is the wire coordinate, σ the complex induced charge distribution, and \mathbf{J} the complex induced current distribution with $\mathbf{J}(\mathbf{x}, t) = \text{Re}\{\mathbf{J}_0(\mathbf{x})e^{-i\omega t}\}$. The vector $Q_\alpha = Q_{\alpha\beta}n_\beta$ with components in the backscattering direction $\hat{\mathbf{n}}$ from the quadrupole moment tensor $Q_{(\alpha\beta)}$ can be written as

$$\mathbf{Q}(\hat{\mathbf{n}}, t) = 3 \int_{V'} \mathbf{x}' (\hat{\mathbf{n}} \cdot \mathbf{x}') \sigma(\mathbf{x}', t) d\mathbf{x}'. \quad (3)$$

Multipoles higher than the quadrupole are less physically intuitive. For the multipole moments we derive snapshots in time as previously for $\sigma(\mathbf{x}, t)$.

Rather than extrapolating the electric field, we calculate it explicitly for these induced moments. We approximate the far-field electric field \mathbf{E}_{sc} , by electric field vectors from each of the

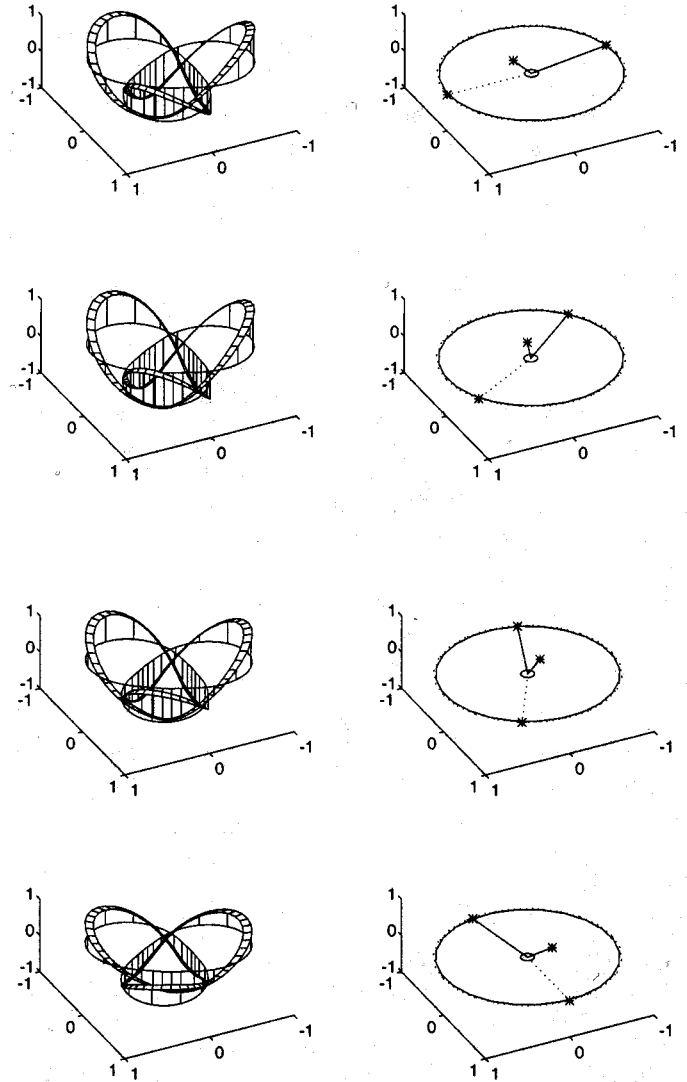


Fig. 4. Time sequence of induced charge distribution (left column) and incident field electric vector (dashed line, right column) and induced electric dipoles (solid lines, right column) for a large untrefoil when the charge resembles a standing wave pattern.

three moments, \mathbf{p} , \mathbf{m} , and \mathbf{Q} in the direction $\hat{\mathbf{n}}$. The backscattering cross section when $\mathbf{E}_{\text{inc}} = E_{\text{inc}}\hat{\mathbf{e}}_0$ becomes

$$\frac{d\sigma}{d\Omega}(\hat{\mathbf{n}}, \hat{\mathbf{e}}; -\hat{\mathbf{n}}, \hat{\mathbf{e}}_0) = \frac{1}{E_{\text{inc}}^2} \left| \frac{k^2}{4\pi\epsilon_0} \hat{\mathbf{e}}^* \cdot \mathbf{p} - \frac{k^2}{4\pi} \left(\frac{\mu_0}{\epsilon_0} \right)^{\frac{1}{2}} \hat{\mathbf{e}}^* \cdot (\hat{\mathbf{n}} \times \mathbf{m}) - \frac{ik^3}{24\pi\epsilon_0} \hat{\mathbf{e}}^* \cdot \mathbf{Q}(\hat{\mathbf{n}}) \right|^2 \quad (4)$$

where k is the wavenumber and r the radial distance to the observation point along $\hat{\mathbf{n}}$. The direction of the field from the electric dipole is $(\hat{\mathbf{n}} \times \mathbf{p}) \times \hat{\mathbf{n}}$, that from the magnetic dipole is $\hat{\mathbf{n}} \times \mathbf{m}$, and that from the electric quadrupole is $\hat{\mathbf{n}} \times (\hat{\mathbf{n}} \times \mathbf{Q}(\hat{\mathbf{n}}))$. We use each term to estimate the importance of the moments' relative contributions to the structure's backscattering cross section and effect on polarization. Examples of such backscattering cross sections are given in Table I.

TABLE I
BACKSCATTERING CROSS SECTIONS FOR SMALL ($kL = 0.01$) AND LARGE ($kL = 1.5$) STRUCTURES. FOR EACH STRUCTURE WE SHOW THE DIFFERENTIAL BACKSCATTERING CROSS SECTION FOR THE STRUCTURE AND THEN THAT FROM EACH OF THE MOMENTS INDUCED ON THE STRUCTURE (ELECTRIC DIPOLE, MAGNETIC DIPOLE, AND ELECTRIC QUADRUPOLE) FOR CO- AND CROSS-POLARIZATIONS. ALSO SHOWN IS THE PERCENTAGE DUE TO EACH MOMENT. NUMBERS SMALLER THAN 10^{-18} HAVE BEEN REPLACED WITH ZERO

Backscattering Cross-Section	(A)	(B)	(C)	(D)
	Co-polarized	% of total co-	Cross-polarized	% of total cross-
(1) small loop				
total cross-section	0	100	2.6×10^{-14}	100
electric dipole	0	100	2.6×10^{-14}	100
magnetic dipole	0	0	0	0
electric quadrupole	0	0	0	0
(2) large loop				
total cross-section	0	100	2.2×10^{-1}	100
electric dipole	0	100	2.2×10^{-1}	100
magnetic dipole	0	0	0	0
electric quadrupole	0	0	0	0
(3) small trefoil				
total cross-section	0	100	1.7×10^{-15}	100
electric dipole	0	99	1.7×10^{-15}	99
magnetic dipole	0	0	0	0
electric quadrupole	0	0	0	0
(4) small untrefoil				
total cross-section	2.4×10^{-18}	100	1.8×10^{-15}	100
electric dipole	2.3×10^{-18}	96	1.8×10^{-15}	99
magnetic dipole	0	0	0	0
electric quadrupole	0	0	0	0
(5) large trefoil				
total cross-section	0	100	5.6×10^{-2}	100
electric dipole	0	90	6.4×10^{-2}	115
magnetic dipole	0	0	3.1×10^{-5}	0
electric quadrupole	0	0	3.7×10^{-5}	0
(6) large untrefoil				
total cross-section	3.2×10^{-4}	100	5.8×10^{-2}	100
electric dipole	9.7×10^{-5}	31	6.0×10^{-2}	104
magnetic dipole	1.4×10^{-5}	4	7.1×10^{-7}	0
electric quadrupole	6.3×10^{-5}	20	1.4×10^{-5}	0

We find that the behavior of the electric fields radiated by the moments always divides the structures into the same groups that the backscattering polarization does: those with rotational symmetry ($N > 2$) about the scattering axis and those without.

A. Trefoil: Symmetric Knot

For the rotationally symmetric trefoil, the calculated electric dipole behaves like the dipole derived for the loop. It rotates circularly in the plane perpendicular to $\hat{n} = -\hat{n}_0$, which is also the axis of symmetry, and has the same rotational frequency as the incident field. As described above, along the backscattering axis this dipole radiates an electric field which is circularly polarized. In particular, it is purely cross polarized for the backscattering direction.

The radiated electric fields are not as easily derived for the magnetic dipole and electric quadrupole, so we calculate them directly rather than examining the moments. For each moment, the electric field vector in the far zone is perpendicular to \hat{n} and rotates circularly at the incident field frequency, qualitatively like the electric dipole field. Therefore, the magnetic dipole and electric quadrupole also yield only cross-polarized radiation in the backscatter direction. None of the three moments

contribute copolarized radiation. For the cases considered: there is often a magnitude difference between the electric fields from the three moments, so they contribute with different weights to the backscattering cross section.

B. Untrefoil: Asymmetric Unknot

The circularly polarized incident field also induces a rotating electric dipole on the untrefoil, but this dipole traces an ellipse rather than a circle. The elliptical motion means that though the period of rotation is the same as for the incident electric field vector, the phase difference between the incident field electric vector and the induced dipole is sinusoidal, not constant, and its magnitude varies sinusoidally. This dipole rotates in the plane perpendicular to the scattering direction. Since circularly rotating dipoles are directly related to circular polarization, we use them rather than linearly oscillating components to decompose the elliptical dipole. This yields two circular dipoles of different magnitudes rotating with opposite frequencies. The larger circular component rotates synchronously with the elliptical vector and the smaller rotates counter to it. Each component radiates a circularly polarized electric field. If the elliptical dipole rotates with the incident electric vector, the larger component will

produce cross polarization, the smaller copolarization. This elliptical dipole contributes more to cross polarization. If it rotates in the opposite direction, then the larger circular component gives co-polarization and the smaller gives cross-polarization. Alternatively, one can directly calculate the electric field from the dipole moment. This result is an elliptically rotating electric field vector that decomposes directly to both polarizations.

Since there is a nonzero counter rotating component (above the noise), co-polarized backscattering exists. This gives some physical motivation for the presence of both polarizations in backscattering from untrefolds. Unlike the planar loop unknot, these unknots bear an induced charge distribution whose dipole moment rotates elliptically. Extrapolating from the planar loop, however, the source for the dipole and co-polarized backscattering can be conceptualized as a counter-rotating charge distribution.

As with the trefoil, we calculate the electric field for the magnetic dipole and electric quadrupole moments induced on the untrefold. For both cases, as for the electric dipole, fields rotate elliptically with the same period as the incident electric field. These ellipses are in some cases highly eccentric; circular decomposition gives two counter-rotating components that are comparable in magnitude. This elliptical field contains both polarizations with similar weights. In many cases the elliptical electric field vectors from these moments rotate with the opposite sense, contributing more co- than cross-polarized backscatter.

C. Morph: Asymmetric Knots and Unknots

The set of morphs includes knots that are topologically identical to trefoils. They are also geometrically similar, but they do not possess rotational symmetry. Included in this set are unknots topologically equivalent to the untrefold. These are geometrically similar as well and are asymmetric.

For all morphs, the electric dipole moment and the electric fields from the magnetic dipole and electric quadrupole moments resemble those for the untrefold. They all rotate elliptically and contribute to both polarizations in backscattering. This holds whether the morph is topologically a trefoil or an untrefold. The knotted morph scatters like the unknotted untrefold and the knotted trefoil like the unknotted loop. The defining characteristic is rotational symmetry. This clarifies the results for the loop, trefoil, and untrefold in terms of the effect of symmetry and topology on the resulting backscattering polarizations and induced moments.

We see that circularly polarized waves induce on symmetric objects an electric dipole moment that rotates circularly. The magnetic dipole and electric quadrupole moments radiate fields that also rotate circularly. On asymmetric objects, the same waves induce an electric dipole moment that rotates elliptically. Here, the electric fields from the magnetic dipole and electric quadrupole rotate elliptically. Referring to only the simplest level treated here, since the electric dipole moments induced on asymmetric structures contain counter-rotating components, we see that the scatterer's asymmetry changes the polarization of the incident wave.

The electric fields of the first three moments all display the same general behavior, so we need only consider the electric dipole to obtain qualitative information about polarization. For some cases studied here, the electric dipole is also quantitatively accurate, generally for small to moderate sizes. For all sizes of the planar loop studied here, the electric dipole accounts for most of the backscattering cross-section, as seen in Table I, the first two sections. (Again, the very small numbers indicate results that should theoretically be zero, but numerical noise prevents this.) Here, the magnetic dipole and electric quadrupole backscattering cross-sections are insignificant.

For more complicated structures that are still electrically small [Table I, section (3) and (4)], the backscattering cross-section from the induced electric dipole still represents a large percentage of the structure's backscattering cross section. However, the cross sections from the magnetic dipole and electric quadrupole rapidly grow with the size of the structure in contrast to the loop case. Even with larger structures, the electric dipole rotation still correlates with the polarization, circular rotation associated with cross-polarization, and elliptical with mixed polarization. As indicated by the percentages [Table I, section (5) and (6)], the backscattering cross section can no longer be accounted for through the electric dipole by itself; the magnetic dipole and electric quadrupole become important, as well as other moments.

In summary, the field of the electric dipole illustrates a range of behaviors sufficient to physically motivate the resulting polarization of the backscatter. For symmetric objects, its electric field vector rotates circularly. For asymmetric objects it rotates elliptically. This is true for all sizes of structures. The motion of the electric fields from the magnetic dipole and electric quadrupole is consistent with this qualitative picture. For small structures, the electric dipole is also quantitatively useful. For larger structures, the electric dipole is less dominant and the two higher moments become important, particularly for asymmetric objects.

V. CONCLUSION

We examine the differential backscattering cross section from knots and unknots. In cases with appreciable co- and cross-polarized cross sections, the structure is asymmetric and the induced electric dipole moment has two counter-rotating circular components. When cross-polarization dominates with the co-polarized component in the numerical noise, the structure is symmetric and the induced electric dipole has a single circular component rotating synchronously with the incident electric field vector. The magnetic dipole and electric quadrupole moments radiate electric field vectors that display similar behavior. Extrapolating from the circular loop, we suggest a counter-rotating charge distribution as a canonical physical source for the counter-rotating moments.

The electric dipole is deterministic in the sense that its rotation correlates with the polarization of the backscatter, elliptical motion when the backscattered radiation is both co- and cross-polarized, and circular and synchronous when backscattering is purely cross-polarized. For small structures, the electric dipole also dominates quantitatively; for larger ones, it does

not. However, the behavior of the electric fields from the magnetic dipole and the electric quadrupole does not add anything qualitatively new to the electric dipole picture. Like the electric dipole, these other moments do not provide a complete picture outside of the low frequencies. For simplicity and physical insight, the electric dipole is the most useful moment.

The examination of electric dipoles of the induced charge distributions expands our physical understanding of backscattering from trefoils and untrefoils. We pursue such conceptualization with an eye toward future detection of and subsequent understanding of differences in scattering from such knots and unknots that exist in both nature and in man-made structures. One possible reason for interest is the characterization of large molecules, particularly those with biological importance. The trefoil occurs naturally in long molecules, and specifically in one of the most interesting biomolecules, DNA [9]–[11].

ACKNOWLEDGMENT

Portions of this work were presented at conferences [12]–[14]

REFERENCES

- [1] M. Kac, "Can one hear the shape of a drum?," *Amer. Math. Monthly*, vol. 73, no. 4, pp. 1–24, 1966.
- [2] D. L. Jaggard and O. Manuar, "Can one 'hear' the handedness or topology of a knot?," in 1995 AP-S/URSI Meeting, Newport Beach, CA, June 1995, presented.
- [3] O. Manuar and D. L. Jaggard, "Backscatter signature of knots," *Opt. Lett.*, vol. 20, pp. 115–117, Jan. 15, 1995.
- [4] C. E. Baum and H. N. Kritikos, "Symmetry in electromagnetics," in *Electromagnetic Symmetry*, C. E. Baum and H. N. Kritikos, Eds. Washington, DC: Taylor & Francis, 1995, ch. 1, p. 21.
- [5] R. F. Harrington, *Field Computation by Moment Methods*. New York: Macmillan, 1968, p. 63.
- [6] C. F. Bohren and D. R. Huffman, *Absorption and Scattering of Light by Small Particles*. New York: Wiley, 1983, p. 121.
- [7] J. D. Jackson, *Classical Electrodynamics*, 2nd ed. New York: Wiley, 1975, ch. 9, p. 412, footnote.
- [8] —, *Classical Electrodynamics*, 2nd ed. New York: Wiley, 1975, ch. 9, p. 395.
- [9] T. Schlick and W. K. Olson, "Trefoil knotting revealed by molecular dynamics simulations of supercoiled DNA," *Sci.*, vol. 257, pp. 1110–1115, 1992.
- [10] S. M. Du, B. D. Stollar, and N. C. Seeman, "A synthetic DNA molecule in three knotted topologies," *J. Amer. Chem. Soc.*, vol. 117, pp. 1194–1200, 1995.
- [11] I. Peterson, "Tying knots to tubular geometry, DNA loops," *Science News* 150, vol. 310, Sept. 16, 1996.
- [12] D. L. Jaggard and O. Manuar, "On knots and knotted media," presented at the XXV General Assembly of the International Union of Radio Science, Lille, France, Aug. 28, 1996.
- [13] O. Manuar and D. L. Jaggard, "Wave interactions with trefoils and untrefoils," presented at the 1996 IEEE AP-S International Symposium and URSI Radio Science Meeting, Baltimore, MD, July 21–26, 1996.
- [14] —, "Knots and unknots: Scattering and perceived symmetry," in *Proc. IEEE Antennas and Propagation Soc. Int. Symp.*, vol. 2, Montreal, Canada, July 13–18, 1997, pp. 1464–1467.



Omar Manuar was born in 1967, in Bethesda, MD. From 1985 to 1989, he studied Biophysics at Johns Hopkins University, Baltimore, MD. He is working toward the Ph.D. degree in Molecular Biophysics at the University of Pennsylvania in Philadelphia.

His dissertation research involves the effects of the topology and symmetry of wire loops on electromagnetic wave scattering. His current interests revolve around PC computer hardware and Linux.



Dwight L. Jaggard (S'68–M'77–SM'86–F'91) received the B.S.E.E. and M.S.E.E. degrees from University of Wisconsin–Madison and the Ph.D. degree in electrical engineering and applied physics, California Institute of Technology, Pasadena, in 1971, 1972, and 1976, respectively.

Since 1980, he has been with the Moore School of Electrical Engineering, University of Pennsylvania, Philadelphia, as Professor of Electrical Engineering. He is co-founder of the Complex Media Laboratory and has performed research in electromagnetics and

optics with an emphasis on waves and complex media and methods of inverse scattering and imaging. His current research is involved with the fundamentals and applications of fractal electrodynamics, electromagnetic chirality, and the effects of symmetry and topology on waves in knotted media.

Professor Jaggard received the S. Reid Warren Award for Distinguished Teaching and the Christian F. and Mary R. Lindback Award for Distinguished Teaching. He is a Fellow of the Optical Society of America. He has served as an editor of the *Journal of Electromagnetic Wave Applications* and editor of several special sections of the *Journal of the Optical Society* and the PROCEEDINGS OF THE IEEE and served as Associate Editor of the IEEE TRANSACTIONS ON ANTENNAS AND PROPAGATION. He has contributed to and is co-editor of *Recent Advances in Electromagnetic Theory* (Springer-Verlag, New York; Berlin, Germany; Vienna, Austria, 1990), and contributor to *Symmetry in Electromagnetics* (Taylor & Francis, New York, 1995), *Fractals in Engineering*, (Springer-Verlag, New York; Berlin, Germany; Vienna, Austria, 1997); *Fractals: Theory and Applications in Engineering* (Springer-Verlag, New York; Berlin, Germany; Vienna, Austria, 1999); and *Frontiers of Electromagnetics* (IEEE Press, Piscataway, NJ, 2000). He has also served as a consultant to government and industry.